Journal of Photochemistry and Photobiology A: Chemistry 217 (2011) 356–362

Contents lists available at ScienceDirect

Journal of Photochemistry and Photobiology A: Chemistry

journal homepage: www.elsevier.com/locate/jphotochem

Preparation of pyrene-functionalized fluorescent film with a benzene ring in spacer and sensitive detection to picric acid in aqueous phase

Haiying Du, Gang He, Taihong Liu, Liping Ding, Yu Fang*

Key Laboratory of Applied Surface and Colloid Chemistry (Ministry of Education), School of Chemistry and Materials Science, Shaanxi Normal University, Xi'an 710062, PR China

ARTICLE INFO

Article history:
Received 21 August 2010
Received in revised form 21 October 2010
Accepted 5 November 2010
Available online 13 November 2010

Keywords:
Pyrene
Nitroaromatics
Picric acid
Film sensor
Fluorescence

ABSTRACT

A fluorescent sensing film was fabricated by chemical assembling pyrene moieties on a glass plate surface via a spacer containing a benzene ring. The film was used for the detection of nitroaromatic compounds (NACs), particularly picric acid (PA), in aqueous phase. Introduction of benzene structure in the spacer favors π–π stacking between pyrene moieties on the end of each spacer, which encourages direct exposure of the fluorophore residues to aqueous phase, and thus the film is able to quickly monitor NACs. The advantages of this design have been demonstrated experimentally in terms of the highly sensitive response of the above-mentioned film to the presence of trace amounts of NACs in aqueous solution. The detection limit (DL) of the film to PA reaches 1.0×10^{-8} mol/L. Further experiments demonstrated that the sensing process is fully reversible and is free of interference from common chemicals like toluene, benzene, trichlormethane, ethanol, artificial seawater, NaOH, HCl, etc. Furthermore, fluorescence lifetime measurement revealed that the quenching is static in nature.

1. Introduction

Contamination of soil and water at sites where nitroaromatic compounds (NACs) are manufactured or used is a serious environmental problem because ingestion of them may cause impair vision, liver or kidney damage, gastritis, aplastic anemia, cyanosis, dermatitis, etc. [1,2]. Therefore, fast, sensitive and low cost detection of NACs, in particular picric acid (PA), 2,4,6-trinitrotoluene (TNT), 2,4-dinitrotoluene (DNT), and nitrobenzene (NB), in soil and aqueous phase is of great interest. Up to now, various methods such as canines [3], gas chromatography coupled with mass spectrometry [4], high-pressure liquid chromatography [5], surface enhanced Raman spectrometry [6], and electrochemical method [7,8] have been developed for the detection of NACs in liquid phase. Although these techniques are effective, some need to handle with complex sample preparation, some are expensive and time-consuming, and others are difficultly fielded in small, low-power package. Compared with the above mentioned techniques, fluorescent film sensors have gained great attention because of their high sensitivity and selectivity, multiple choices in signals or parameters, and low cost in instrumentation. Furthermore, films sensors are easy to be made into devices, and in theory, they are re-usable and contamination free. Clearly, these advantages must benefit on site analysis.

Among fluorescent film sensors [9–11], both conjugated polymers (CPs) and fluorescent aromatics have been used as sensing elements. Compared with aromatics-based films, CPs-based films are more sensitive even though they are, generally speaking, more difficult to be prepared. However, these films, except a few ones reported by our group, are prepared by using spin-coating, dip-coating or other physical methods, and thereby suffer from issues such as fluorophore leaking, thickness control, and inner-layer analyte diffusion [11–14].

Different from what occurs in CPs-based film sensors, the response of fluorescent sensing films fabricated in a self-assembled monolayer (SAMs) way is significantly faster due to direct exposure of fluorophore moieties, avoiding, at least in principle, inner-layer diffusion problem encountered by CPs-based physically fabricated sensing films. Reinhoudt and co-workers prepared some fluorescent sensing films via immobilizing dansyl, pyrene, or coumarin on glass plate surfaces in a SAMs way. It was reported that those films are highly sensitive and selective to β-cyclodextrin, Na^+, or Pb^{2+} [15–17]. Gulino and co-workers reported a sensitive, reversible, and fast response optical NO_2 sensor via covalently binding porphyrin molecules onto silica substrate [18]. Recently, similar strategy has been employed by Raymo and co-workers to prepare fluorescent sensing films for dopamine of catecholamine neurotransmitters [19]. The principles behind the sensing is that the association of the 2,7-diazapyrenium, which is the sensing element and functions as an acceptor, with dopamine, a donor, via charge–transfer interaction produces a fluorescence quenching at the solid–liquid interface.

Over the past decade, our group has been seeking to develop a new family of fluorescent sensing films via a SAMs way and has realized sensitive and selective detection of NACs in vapor phase

* Corresponding author. Tel.: +86 29 85310081; fax: +86 29 85307566.
E-mail address: yfang@snnu.edu.cn (Y. Fang).

1010-6030/$ – see front matter © 2010 Elsevier B.V. All rights reserved.
doi:10.1016/j.jphotochem.2010.11.004

and of other analytes in solution [20–23]. It is to be noted that the structures of the spacers connecting the sensing elements and the substrates have played important roles for the performances of the films. Moreover, in studies of low-molecular mass organic gelators, our group found that introduction of a simple benzene ring in the spacer of two cholesteryl units resulted in a great effect upon their assembling behaviors in solution [24]. Illuminated by this work and considering the importance of spacer structure to the performance of a fluorescent film sensor, and the fact that all SAMs based fluorescent sensing films reported till now do not contain aromatic structures within their spacers, a novel fluorescent film has been specially designed by employing a spacer containing a benzene ring. It was expected that introduction of a benzene structure in the spacer may cause a significant effect upon its fluorescent and sensing behaviors. This paper reports the details of the fabrication of a pyrene-functionalized fluorescent film with a benzene structure in the spacer connecting the fluorophore and a substrate, glass plate, and its sensing behavior to PA in aqueous phase.

2. Experimental

2.1. Reagents

Pyrenesulfonyl chloride (PSC) was synthesized by adopting a literature method [25]. p-Xylylenediamine (PXDA; TCI, >99%) and 3-glycidoxypropyltrimethoxysilane (GPTS; Acros, 97%) were used directly without further purification. Other chemicals used are of the highest grade commercially available, and also used directly without further purification. Water used throughout is de-ionized and then double distilled. NACs including TNT, DNT, NB and PA were of analytical grade and used directly without further purification. (**Caution**: *TNT and other NACs used in the present study are highly explosive and should be handled only in small quantities.*)

2.2. Measurements

Pressed KBr disks for the powder samples were used for the transmission infrared spectroscopy measurements, and their FTIR spectra were obtained with a Bio-Rad FTIR spectrometer. X-ray photoelectron spectroscopy (XPS) measurements were carried out on an ESCAPHI5400 photoelectron spectrometer using a monochromatic Mg Kα X-ray source. Contact angles of the films were measured on a dataphysics OCA20 contact-angle system at ambient temperature. Fluorescence measurements were performed at room temperature on a time-correlated single photon counting Edinburgh FLS 920 fluorescence spectrometer with a front-face method. The fabricated film was inserted into a quartz cell with its surface facing the excitation light source. The position of the film was kept constant during each set of measurements.

2.3. Synthesis of N-1-pyrenesulfonyl-p-xylylenediamine (PSPXDA)

PSPXDA was prepared by adopting a modified literature method [23,25]. The resulting solution was kept as PSPXDA solution and used directly in the following surface assembling.

For characterization, PSPXDA was isolated from the above solution in its salt form by acidification of the solution with 0.1 mol/L HCl in diethyl ether. The fine buff precipitate was filtered and dried at room temperature. Anal. Calcd. for the salt of PSPXDA $C_{24}H_{21}N_2SO_2Cl$: C, 65.97; H, 4.84; N, 6.41. Found: C, 65.87; H, 4.81; N, 6.95. ^{1}H NMR (300 MHz, DMSO-d_6): δ (ppm) 9.0 (1H), 8.2–8.8 (8H), 7.2 (4H), 4.0 (2H), 3.8 (2H). FTIR (KBr, cm^{-1}): 3049 (m), 1625 (m), 1430 (m), 1319 (s), 1060 (m), 849 (s), 663 (s), 559 (s). Melting point: 241–242 °C.

2.4. Activation and silanization of the glass plate surface

A glass plate (0.9 cm × 2.5 cm) was treated in a "piranha solution" (3/7, V/V, 30% H_2O_2/98% H_2SO_4) [26] (**Warning**: *Piranha solution should be handled with extreme caution because it can react violently with organic matter.*) at 98 °C for 1 h, rinsed thoroughly with plenty of water, and finally dried at 100 °C in a dust-free oven for 1 h. The activated glass plate was immersed in 50 °C toluene solution of GPTS (0.6%, V/V), containing a trace amount of water, for 12 h. The glass plate was rinsed with toluene and trichlormethane, successively, to remove any physisorbed material.

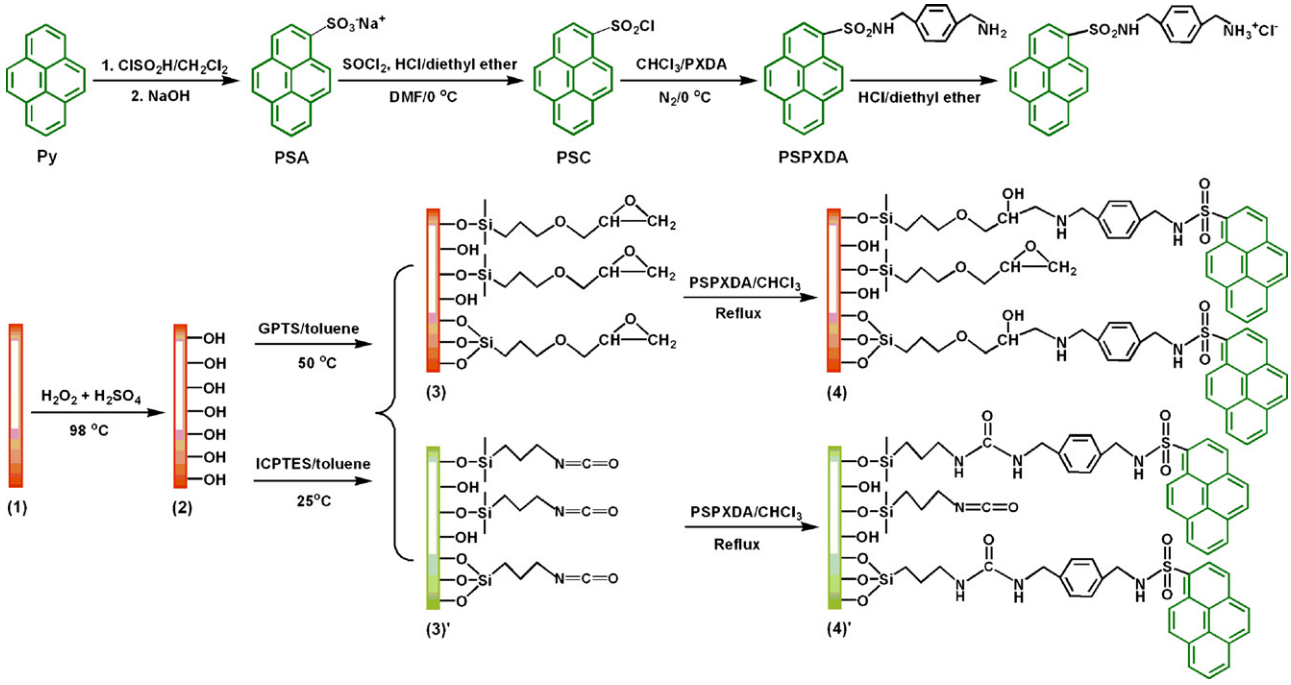

Scheme 1. Schematic representation of the synthesis and immobilization of PSPXDA onto a glass plate surface, and the representative structure of the controlled one.

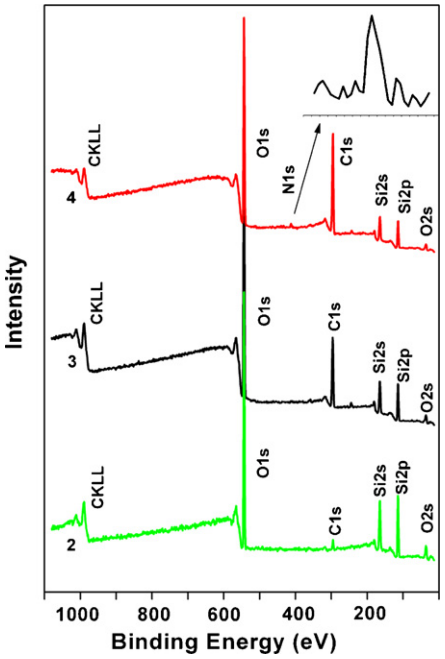

Fig. 1. X-ray photoelectron spectra of the glass plates of various surface structures. The numbers of 2, 3 and 4 stand for the plates of hydroxyl surface, epoxide surface, and pyrene derivatives surface, respectively.

2.5. Chemical coupling of pyrene on the plate surface

The trialkoxysilane-treated glass plate was immerged into a PSPXDA solution in trichlormethane (cf. synthesis of *N*-1-pyrenesulfonyl-p-xylylenediamine) at 61 °C for 12 h. To remove unreacted PSPXDA, the plate was rinsed with plenty of trichlormethane and ethanol, and then extracted with dichloromethane in a Soxhlex extractor for 5 h. The plate was further rinsed with dichloromethane and water, successively, after the extraction. The synthesis of pyrene moieties and its coupling onto a glass plate surface are shown in Scheme 1.

3. Results and discussion

3.1. Film characterization

The films have been characterized by XPS and wettability measurements. Fig. 1 shows the XPS spectra of the substrate of various surface compositions, of which the chemical structures changed from hydroxyl groups to epoxy groups and then to pyrene derivatives along with the treatment. It can be seen that the signal of C1s of the epoxy group covered substrate is much stronger than that of the hydroxyl group covered one, indicating that the silanizing reagent are somewhat exposed to the outer interface. Immobilization of the pyrene moieties on the substrate surface made C1s signal even stronger and the signal of N1s appeared, a strong evidence for the successful coupling of pyrene moieties on the substrate surface. This conclusion is further confirmed by the results from surface wettability measurement.

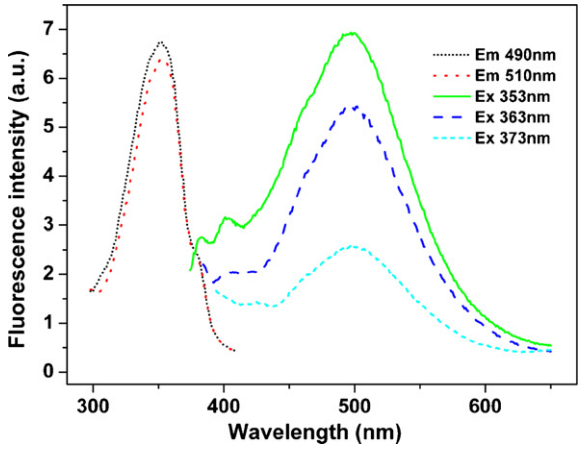

Fig. 3. Fluorescence excitation and emission spectra of the film in aqueous solution.

Contact angles at ambient temperature of the surfaces of the substrates to water at different stages of the functionalization process have been measured and the results are shown in Fig. 2. Reference to the figure reveals that the static contact angle decreased significantly from $10.5 \pm 0.5^\circ$ to $6.9 \pm 0.5^\circ$ after treatment with the "piranha solution". Further treatment with GPTS resulted in a sharp increase in the data ($42.1 \pm 0.8^\circ$), indicating that the wettability of the surface has reversed. The angle increased further after treatment with PSPXDA solution in trichlormethane, and reached a value of $71.1 \pm 0.4^\circ$, a typical hydrophobic surface. These results are consistent with the expectation from the chemical composition of the surface, as shown in Fig. 1 and revealed by XPS measurements.

Success in the chemical coupling of the pyrene moieties on the substrate surface was further investigated by monitoring the fluorescence emission of remained solvent after immersion of the film in trichlormethane for more than 15 h. The fact that no typical pyrene emission was found indicates that the amount of physically adsorbed pyrene moieties is negligible. In other words, pyrene had been chemically coupled on the substrate surface.

3.2. Steady-state excitation and emission spectra of the film

Fig. 3 depicts the steady-state fluorescence excitation and emission spectra of the functional film in aqueous solution as functions of excitation and emission wavelengths. Examination of the figure reveals that the emission is composed of two sharp peaks at wavelengths of 380 nm and 401 nm, and one broad band centered at 500 nm. The peaks and the band can be assigned to pyrene monomer (M) emission and excimer (E) emission, respectively. Similar to the results reported in the literatures [16,27,28], a perfect "sandwich-like" structure may be adopted by the excimer since its maximum emission centers at 500 nm. Furthermore, the excitation spectrum is not varying along with the analysis wavelength increasing to longer wavelength, suggesting that both the excimer emission and the monomer emission originate from fluorophores with similar micro-environment.

Fig. 2. Static contact angles (θ) of various glass plate surfaces and water. The numbers of (1), (2), (3) and (4) have similar meaning with those shown in Scheme 1 and in Fig. 1.

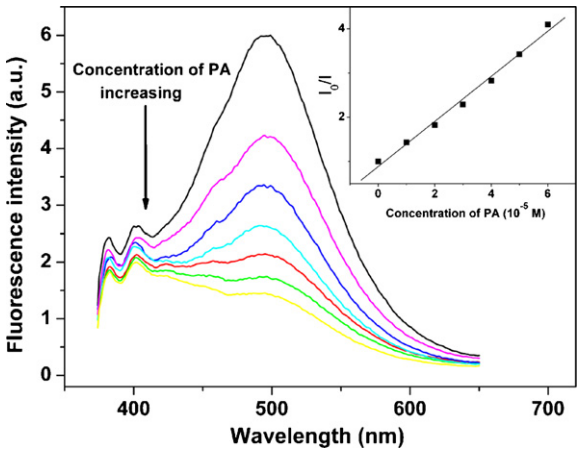

Fig. 4. Fluorescence emission spectra of the film in the presence of PA of different concentrations, which are 0, 1.0, 2.0, 3.0, 4.0, 5.0, 6.0 × 10^{-5} M from top to bottom, respectively (λ_{ex} = 353 nm).

3.3. Fluorescence quenching studies with NACs

As it is well known, NACs are electron poor compounds if compared to that of polycyclic aromatics, and thereby they are effective fluorescence quenchers to most aromatic fluorophores [29]. Accordingly, the effects of commonly found NACs, including TNT, DNT, NB, and PA, to the fluorescence emission of the film were examined. The test has been conducted in the following way: firstly, the film was adhered to one inner-side of a quartz cell with a volume of ca. 3.5 cm^3; secondly, distilled water with a volume of 2.5 cm^3 was added into the cell; and finally, the spectra were recorded when the fluorescence intensity became stable after a certain amount of NAC was injected into the cell. As expected, all the NACs quenched, with different efficiencies, the emission of the film. As an example, Fig. 4 shows the fluorescence emission spectra of the film as a function of the concentration of PA. Clearly, the emission, particularly the excimer emission, of the film decreased significantly with increasing PA concentration. It is to be noted that the position of the excimer emission does not change significantly, indicating that the interaction between the analyte, PA, and the pyrene moieties does not afford emissive states [30]. The fluorescence quenching results can be treated with the Stern–Volmer equation, $I_0/I = 1 + K_{sv}$ [PA], where I_0 and I are the fluorescence intensity of the film in the absence and presence of PA, respectively, and K_{sv} is the Stern–Volmer constant. For the present system, the constant is 5.1 × 10^4 M^{-1}, a value much higher than those of other fluorescent chemosensors for PA, suggesting that the present film may be exploited as an effective film sensor with enhanced sensitivity to PA and other NACs [11,31–36]. Fig. 5 depicts the quenching results of NACs to the fluorescence emission of the film. It can be seen that the film is not only responsible to PA but also to other NACs tested. Each data reported in the figure was recorded 15 min later after the injection of the quencher. It is to be noted that this is not mean that the response of the film to the analyte is slow, but actually the response is much faster because the time required for the equilibration of the quenching is less than 1 min as revealed by time-dependent measurements (cf. Fig. S1). According to the ability of drawing electrons, it is expected that TNT might have the highest quenching efficiency to the emission of the films due to the existence of three nitro-groups on the benzene ring that make the ring have lowest electron density if compared with PA and other NACs [31,36,37]. However, the quenching follows the order of PA > TNT > DNT > NB, rather than TNT > PA > DNT > NB (cf. Fig. 5), suggesting that except PA, for other NACs, electron withdrawing ability dominates the quenching efficiency. The exceptional quenching effect of PA to the fluorescence emission of the film may be explained by considering its acid nature. This is because the three nitro-groups on the benzene ring make the hydroxyl group affixed on the molecular frame behaviors as a modest acid. In contrast, for the present film, there is an imino structure in the spacer, which has a tendency to attract proton, and thereby proton transfer may occur when the film is inserted into the solution of PA. It is the proton transfer that makes PA has a specific affinity to the film. As a result, the local concentration (near the film surface) of the quencher would be significantly higher than that in the bulk phase, which explains why PA is a more efficient quencher than other NACs to the film. To verify this hypothesis, another film of a similar structure but with no imino group in the spacer was specifically fabricated which is designated as film (4)′ (cf. Scheme 1). A similar quenching experiment was also conducted with this film, and it was found: firstly, the quenching efficiency of PA to this film is significantly lower than that to the original film studied; second, for this film, TNT is a more efficient quencher than PA, following the order of pure electron withdrawing ability (cf. inset of Fig. 5). Clearly, all these results indicate that the proton transfer-based specific binding contributed a lot to the extraordinary quenching effect of PA. It is to be noted that introduction of a benzene ring in the spacer does not only compel pyrene moieties extending to the outer side of the film as revealed by the profile of its fluorescence emission spectrum, but also restricts the

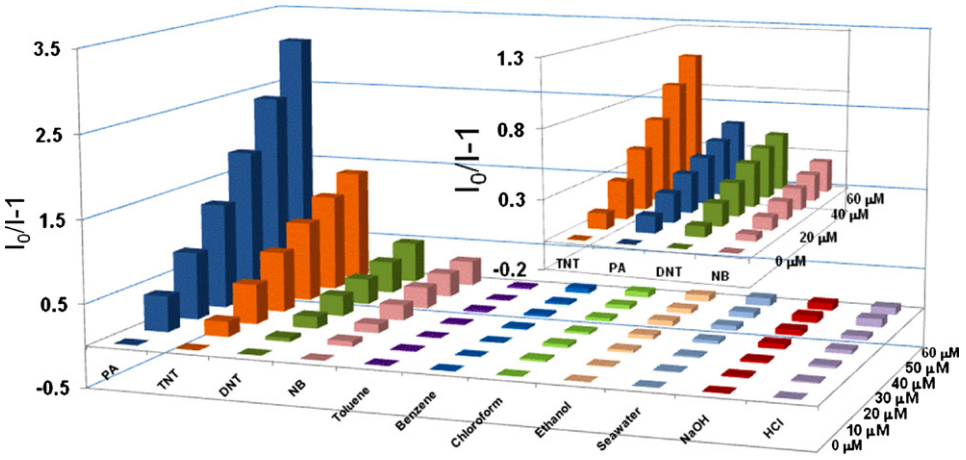

Fig. 5. Quenching results of NACs and commonly found interferents, including toluene, benzene, trichlormethane, ethanol, artificial seawater, NaOH and HCl, to the fluorescence emission of the film with a spacer containing an imino group. Inset: quenching results from control experiments where a similar film has been employed, of which there is no imino group in the spacer.

motions of them (cf. Fig. 3). Similar observations have never been found before in the fluorescence studies of the films with similar structures to the present one. As an example, Figures S2, S3 and S4 show the structure, the fluorescence emission spectrum and the sensing performances to NACs in aqueous phase of one of such films (cf. Supporting Information). These differences may be only attributed to the π–π interaction between benzene rings of neighboring spacers. It is this interaction that restricted the motion of the spacers, and favors excimer formation of neighboring pyrene moieties.

As expected, calculation of the detection limit (DL) once again proved that the response of the film to PA is super-sensitive. The DL for this analyte is 1.0×10^{-8} mol/L, a value quite close to that of 6.0×10^{-9} mol/L and that of 2.1×10^{-8} mol/L reported by Trogler, and our group, respectively. Moreover, the film employed by Trogler's group and that by our group before were all fabricated in a physical way with polysilole or aggregated hexaphenylsilole (HPS) as sensing elements, both suffer from a stability problem [11,38]. The super-sensitivity of this film to PA must be attributed to the specific design of the film, of which a benzene structure had been specially introduced into the spacer. The DL of the film to PA has been determined according to the following functions:

$$s_b = \sqrt{\frac{\sum_{i=1}^{n}(x_i - \bar{x})^2}{n-1}} \quad (1)$$

$$S = \frac{\Delta I}{\Delta c} \quad (2)$$

$$\mathrm{DL} = \frac{3s_b}{S} \quad (3)$$

The standard deviation (s_b) was calculated by measuring the intensity of the film in blank solution for more than 10 times and then got the average intensity ($\bar{x}$) firstly. By fitting the data into function 1, the value of standard deviation (s_b) was obtained. Secondly, a certain amount of PA was added into the blank solution and the resulting variation of the intensity (ΔI) was recorded. By fitting the data into function 2, where Δc is the variation of quencher concentration, the value of precision S was calculated. Finally, the DL was calculated according to function 3.

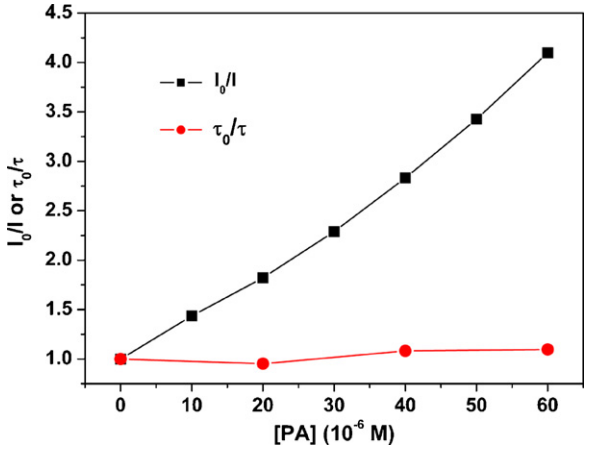

Fig. 6. Plots of I_0/I and τ_0/τ against the concentrations of PA ($\lambda_{ex}/\lambda_{em}$ = 353/500 nm).

3.4. Quenching mechanism of the sensing process

The results from lifetime measurements were illustrated in Fig. 6. It is obvious that the lifetime of the sensing molecules does not change obviously with increasing concentration of PA and τ_0/τ is nearly equal to 1, where τ_0 and τ stand for the lifetimes of the surface-bound fluorophore in the absence and presence of the quencher, respectively. This result indicates that the quenching is mainly caused by the formation of a non-fluorescent complex (F–Q) in a ground-state, which is in support of the hypothesis that the film has a specific binding to PA.

Based upon the discussions made at Sections 3.3 and 3.4, a schematic representation of the quenching of PA to the fluorescence emission of the film is presented in Fig. 7.

3.5. Interference from other chemicals

Interestingly, no significant change in fluorescence emission was observed upon exposing the film to common organic solvents, such as toluene, benzene, trichlormethane, ethanol, and their mixtures with water. Furthermore, the aqueous solutions of NaOH or HCl, and artificial seawater have also been tested as interferents, and it is revealed that these solutions show little effect upon the fluorescence emission of the film (cf. Fig. 5).

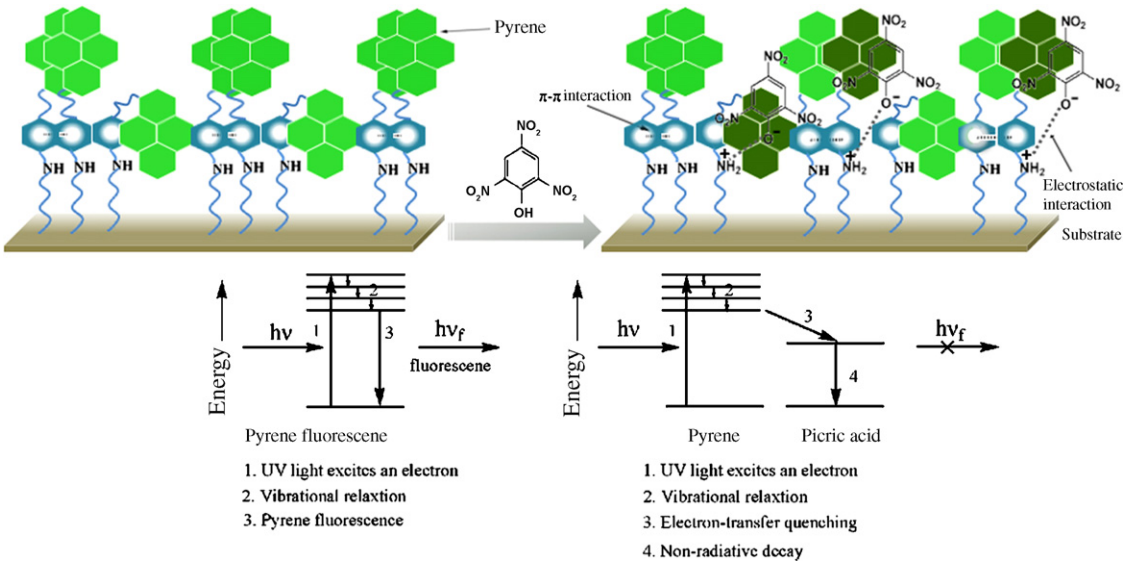

Fig. 7. A schematic representation of the surface enrichment effect of pyrene functionalized film to picric acid and the non-fluorescent complex, pyrene–picric acid, formation.

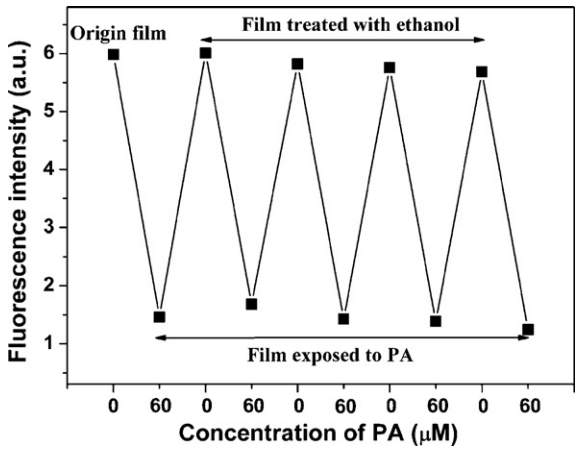

Fig. 8. Results from reversibility measurements, where the fluorescence of the film in pure water and PA solution (6.0×10^{-5} M) was measured alternatively ($\lambda_{ex}/\lambda_{em}$ = 353/500 nm).

3.6. Reversibility of the quenching process

The procedures adopted for examination of the reversibility of the sensing process are as follows: the film was inserted into a cell with 2.5 cm^3 of distilled water, and the fluorescence emission of the film was recorded firstly. Secondly, 60 μL PA solution (2.5×10^{-3} mol/L) was added, and after 10 min equilibration the fluorescence emission of the film was recorded again. Thirdly, after the measurement the film was taken out of the cell, and immersed in an ethanol solution for 15 min and then washed with plenty of distilled water. The film was re-used after the treatment, and the whole process was repeated several times. The results are shown in Fig. 8. It is clear that the response of the film to PA is fully reversible, and furthermore, the film is stable for at least two months provided it is properly preserved. Therefore, it offers opportunity to be made into devices.

4. Conclusion

A stable and bright SAM-based fluorescent film was fabricated with a benzene ring in the spacer. Sensing performance studies demonstrated that the fluorescence emission of the film is sensitive to the presence of NACs, especially PA, with the DL being as low as 1.0×10^{-8} mol/L. Common interferents including toluene, benzene, trichlormethane, ethanol, artificial seawater, NaOH and HCl had little effect upon the emission of the film in aqueous phase. Fluorescence lifetime measurements revealed that the quenching is static in nature. Furthermore, the quenching is fully reversible.

Acknowledgements

We thank the Ministry of Science and Technology of China (No. 2007AA03Z349), the Natural Science Foundation of China (Nos. 20773083, 20803046 and 20927001).

Appendix A. Supplementary data

Supplementary data associated with this article can be found, in the online version, at doi:10.1016/j.jphotochem.2010.11.004.

References

[1] R. Mantha, K.E. Taylor, N. Biswas, J.K. Bewtra, A continuous system for Fe^0 reduction of nitrobenzene in synthetic wastewater, Environ. Sci. Technol. 35 (2001) 3231–3236.
[2] F.D. Marvin-Sikkema, J.A.M. de Bont, Degradation of nitroaromatic compounds by microorganisms, Appl. Microbiol. Biotechnol. 42 (1994) 499–507.
[3] A.W. Czarnik, A sense for landmines, Nature 394 (1998) 417–418.
[4] K. Hakansson, R.V. Coorey, R.A. Zubarev, V.L. Talrose, P. Hakansson, Low-mass ions observed in plasma desorption mass spectrometry of high explosives, J. Mass Spectrom. 35 (2000) 337–346.
[5] D.S. Moore, Instrumentation for trace detection of high explosives, Rev. Sci. Instrum. 75 (2004) 2499–2512.
[6] J.M. Sylvia, J.A. Janni, J.D. Klein, K.M. Spencer, Surface-enhanced Raman detection of 2,4-dinitrotoluene impurity vapor as a marker to locate landmines, Anal. Chem. 72 (2000) 5834–5840.
[7] R.J. Dijkstra, A.N. Bader, G.P. Hoornweg, U.A.T. Brinkman, C. Gooijer, On-line coupling of column liquid chromate graphy and Raman spectroscopy using a liquid core waveguide, Anal. Chem. 71 (1999) 4575–4579.
[8] R. Hodyss, J.L. Beauchamp, Multidimensional detection of nitroorganic explosives by gas chromatography–pyrolysis-ultraviolet detection, Anal. Chem. 77 (2005) 3607–3610.
[9] D.T. McQuade, A.E. Pullen, T.M. Swager, Conjugated polymer-based chemical sensors, Chem. Rev. 100 (2000) 2537–2574.
[10] K.J. Albert, N.S. Lewis, C.L. Schauer, G.A. Sotzing, S.E. Stitzel, T.P. Vaid, D.R. Walt, Cross-reactive chemical sensor arrays, Chem. Rev. 100 (2000) 2595–2626.
[11] G. He, H.N. Peng, T.H. Liu, M.N. Yang, Y. Zhang, Y. Fang, A novel picric acid film sensor via combination of the surface enrichment effect of chitosan films and the aggregation-induced emission effect of siloles, J. Mater. Chem. 19 (2009) 7347–7353.
[12] J.S. Yang, T.M. Swager, Porous shape persistent fluorescent polymer films: an approach to TNT sensory materials, J. Am. Chem. Soc. 120 (1998) 5321–5322.
[13] S.W. Thomas III, G.D. Joly, T.M. Swager, Chemical sensors based on amplifying fluorescent conjugated polymers, Chem. Rev. 107 (2007) 1339–1386.
[14] Y.Y. Long, H.B. Chem, Y. Yang, H.M. Wang, Y.F. Yang, N. Li, K. Li, J. Pei, F. Liu, Electrospun nanofibrous film doped with a conjugated polymer for DNT fluorescence sensor, Macromolecules 42 (2009) 6501–6509.
[15] M. Crego-Calama, D.N. Reinhoudt, New materials for metal ion sensing by self-assembled monolayers on glass, Adv. Mater. 13 (2001) 1171–1174.
[16] N.J. van der Veen, S. Flink, M.A. Deij, R.J.M. Egberink, F.C.J.M. van Veggel, D.N. Reinhoudt, Monolayer of a Na^+-Selective fluoroionophore on glass: connecting the fields of monolayers and optical detection of metal ions, J. Am. Chem. Soc. 122 (2000) 6112–6113.
[17] S. Flink, F.C.J.M. van Veggel, D.N. Reinhoudt, A self-assembled monolayer of a fluorescent guest for the screening of host molecules, Chem. Commun. (1999) 2229–2230.
[18] A. Gulino, P. Mineo, E. Scamporrino, D. Vitalini, I. Fragala, Molecularly engineered silica surfaces with an assembled porphyrin monolayer as optical NO_2 molecular recognizers, Chem. Mater. 16 (2004) 1838–1840.
[19] M.A. Cejas, F.M. Raymo, Fluorescent diazapyrenium films and their response to dopamine, Langmuir 21 (2005) 5795–5802.
[20] S.J. Zhang, F.T. Lü, L.N. Gao, L.P. Ding, Y. Fang, Fluorescent sensors for nitroaromatic compounds based on monolayer assembly of polycyclic aromatics, Langmuir 23 (2007) 1584–1590.
[21] H.H. Li, J.P. Kang, L.P. Ding, F.T. Lü, Y. Fang, A dansyl-based fluorescent film: preparation and sensitive detection of nitroaromatics in aqueous phase, J. Photochem. Photobiol. A: Chem. 197 (2008) 226–231.
[22] F.T. Lü, L.N. Gao, L.P. Ding, L.L. Jiang, Y. Fang, Spacer layer screening effect: a novel fluorescent film sensor for organic copper(II) salts, Langmuir 22 (2006) 841–845.
[23] L.N. Gao, Y. Fang, X.P. Wen, Y.G. Li, D.D. Hu, Monomolecular layers of pyrene as a sensor to dicarboxylic acids, J. Phys. Chem. B 108 (2004) 1207–1213.
[24] M. Xue, K.Q. Liu, J.X. Peng, Q.H. Zhang, Y. Fang, Novel dimeric cholesteryl-based $A(LS)_2$ low-molecular-mass gelators with a benzene ring in the linker, J. Colloid Interface Sci. 327 (2008) 94–101.
[25] S.A. Ezzell, C.L. McCormick, Synthesis and solution characterization of pyrene-labeled polyacrylamides, in: S.W. Shalaby, C.L. McCormick, G.B. Butler (Eds.), Water-Soluble Polymers, ACS Symposium Series, Washington, DC, 1991, pp. 130–150.
[26] F.S. Xiao, M. Ichikawa, Oxide-supported triruthenium ketenylidene cluster: evidence for metal–metal bonds from laser Raman spectroscopy, Langmuir 9 (1993) 2963–2964.
[27] F.M. Winnik, Photophysics of preassociated pyrenes in aqueous polymer solutions and in other organized media, Chem. Rev. 93 (1993) 587–614.
[28] J. Matsui, M. Mitsuishi, T. Miyashita, A study on fluorescence behavior of pyrene at the interface of polymer Langmuir–Blodgett films, J. Phys. Chem. B 106 (2002) 2468–2473.
[29] S. Glazier, J.A. Barron, N. Morales, A.M. Ruschak, P.L. Houston, H.D. Abrun, Quenching dynamics of the photoluminescence of $[Ru(bpy)3]^{2+}$-pendant PAMAM dendrimers by nitro aromatics and other materials, Macromolecules 36 (2003) 1272–1278.
[30] Y. Liu, R.C. Mills, J.M. Boncella, K.S. Schanze, Fluorescent polyacetylene thin film sensor for nitroaromatics, Langmuir 17 (2001) 7452–7455.
[31] H. Sohn, M.J. Sailor, D. Magde, W.C. Trogler, Detection of nitroaromatic explosives based on photoluminescent polymers containing metalloles, J. Am. Chem. Soc. 125 (2003) 3821–3830.
[32] R.Y. Tu, B.H. Liu, Z.Y. Wang, D.M. Gao, F. Wang, Q.L. Fang, Z.P. Zhang, Amine-capped ZnS–Mn^{2+} nanocrystals for fluorescence detection of trace TNT explosive, Anal. Chem. 80 (2008) 3458–3465.
[33] P. Lu, J.W.Y. Lam, J.Z. Liu, C.K.W. Jim, W.Z. Yuan, N. Xie, Y.C. Zhong, Q. Hu, K.S. Wong, K.K.L. Cheuk, B.Z. Tang, Aggregation-induced emission in a

hyperbranched poly(silylenevinylene) and superamplification in its emission quenching by explosivesa, Macromol. Rapid Commun. 31 (2010) 834–839.
[34] Z. Li, Y.Q. Dong, J.W.Y. Lam, J.X. Sun, A.J. Qin, M. Häußler, Y.P. Dong, l.D. Sung, H.H.Y Williams, H.S. Kwok, B.Z Tang, Functionalized siloles: versatile synthesis, aggregation-induced emission, and sensory and device applications, Adv. Funct. Mater. 19 (2009) 905–917.
[35] Y. Zhang, G. He, T.H. Liu, M.N. Yang, L.P. Ding, Y. Fang, Sensing performances of oligosilane functionalized fluorescent film to nitrobenzene in aqueous solution, Sensor Lett. 7 (2009) 1141–1146.
[36] A. Saxena, M. Fujiki, R. Rai, G. Kwak, Fluoroalkylated polysilane film as a chemosensor for explosive nitroaromatic compounds, Chem. Mater. 17 (2005) 2181–2185.
[37] S.J. Toal, W.C. Trogler, Polymer sensors for nitroaromatic explosives detection, J. Mater. Chem. 16 (2006) 2871–2883.
[38] H. Sohn, R.M. Calhoun, M.J. Sailor, W.C. Trogler, Detection of TNT and picric acid on surfaces and in seawater by using photoluminescent polysiloles, Angew. Chem. Int. Ed. 40 (2001) 2104–2105.